

# B Hadron Properties Measured in the DØ Experiment

H. Eugene Fisk

Fermilab, MS357, P.O. Box 500, Batavia, IL 60510 U.S.A.

(On behalf of the DØ Collaboration)

We report on the observation of b-hadron states reconstructed using the DØ detector data at the Tevatron Collider. Measurements of the mass and relative rates of neutral excited  $B_d$  and  $B_s$  mesons, and the discovery of the  $\Xi_b$  baryon are described.

## 1. Introduction

The study of charm and beauty mesons and baryons provides many opportunities to not only measure and classify their spectroscopic states, but also it serves as a testing ground for aspects of flavor QCD such as heavy quark effective theory and lattice gauge calculations, that are used in precise calculations of masses, lifetimes and cross sections. The Fermilab Tevatron has provided both fixed target and proton – antiproton collider facilities that not only account for the discovery of b-quarks but also have dovetailed well with the b-factories to answer a variety of b-physics questions, some of which were not readily explored at existing  $e^+e^-$  and electron-positron colliders. An added feature of the hadron colliders is their large cross-section and high luminosity for production of b-quark states that complements the high luminosities of the b-factories.

## 2. The DØ Experiment

As the Tevatron luminosity has increased, primarily to pursue high  $p_t$  physics issues such as the precise mass measurements of the W boson and the Top quark and searches for the Higgs, additions to the collider detectors have allowed the development of triggers and the ability to log large event samples that now result in a vigorous Tevatron b-physics program. Upgrades to the muon system, the addition of a 2T superconducting solenoid and the DØ silicon and fiber tracking systems have greatly enhanced the experiment's b-physics program.

## 3. Orbitally-excited Neutral $B_d$ mesons

B-quark meson states result from the strong binding of up, down, charmed or strange quarks with b-

quarks. In addition to the established  $B^+$ ,  $B^0$ ,  $B_s$ , and  $B_c$  ground states, quark model calculations predict two broad ( $J^P = 0^+$  and  $1^+$ ) and two narrow ( $1^+$  and  $2^+$ )  $B^*$  states designated  $B_1$  and  $B_2^*$  [1] [2] [3] [4] [5] [6]. The two broad states decay via S-wave with widths of a few hundred  $\text{MeV}/c^2$  that would be difficult to separate from background and two narrow states with a light quark and b quark in a total angular momentum state  $j=3/2$  ( $L=1$ ) that decays via D wave with expected widths of  $\sim 10 \text{ MeV}/c^2$ . These states are observable by their decays to  $B^{+(*)} \pi^-$ :

$$(1) \quad B_1 \rightarrow B^{*+} \pi^-; \quad B^{*+} \rightarrow B^+ \gamma;$$

$$(2) \quad B_2^* \rightarrow B^{*+} \pi^-; \quad B^{*+} \rightarrow B^+ \gamma;$$

$$(3) \quad B_2^* \rightarrow B^+ \pi^-.$$

The direct decay of  $B_1 \rightarrow B^+ \pi^-$  is forbidden due to conservation of angular momentum and parity. Note that charge conjugate modes are implied throughout this article. The  $B^+$  is required to be reconstructed via its decay chain [7]:

$$B^+ \rightarrow J/\psi K^+ \quad \text{with the } J/\psi \rightarrow \mu^+ \mu^-.$$

The two muons must form a common vertex and have an invariant mass in the range 2.80 to 3.35  $\text{GeV}/c^2$ . Note the asymmetric interval above and below the  $J/\psi$ , which is done to avoid the  $\psi'$ . An additional charged track with momentum  $> 0.7 \text{ GeV}/c$  and  $p_t > 0.5 \text{ GeV}/c$ , that makes a common vertex with the  $J/\psi$  decay point, is assigned the  $K$  mass and is required to have a  $\chi^2 < 16$  for three degrees of freedom with the two muons. The primary vertex of the interaction is determined using the

average position of the beam/collision point as a constraint[8]. The displacement of the  $\mu$ - $\mu$ - $K$  vertex from the primary interaction point was required to be  $> 3\sigma$  in the plane transverse to the beam direction, for the event to become a charged  $B$  meson candidate.

To complete the charged  $B$  selection process several variables that are sensitive to the separation of signal from background are combined in a likelihood ratio [9]. The variables used include: (a) the smaller of the transverse momenta of the two muons, (b) the  $B^+$  decay vertex  $\chi^2$ , (c) the  $B^+$  decay length divided by its error, (d) the significance  $S_B$  (see definition below) of the charged  $B$  track impact parameter (used in the likelihood function, but required to be  $< 40$ ), (e) the transverse momentum of the  $K^+$ , and (f) the significance  $S_K$  of the  $K^+$ . Here the significance for a track  $j$ , is defined to be:

$S_j = [\varepsilon_T/\sigma(\varepsilon_T)]^2 + [\varepsilon_L/\sigma(\varepsilon_L)]^2$ , where  $\varepsilon_T$  ( $\varepsilon_L$ ) are the impact parameter projections, with respect to the primary vertex on a plane transverse (parallel) to the beam where  $\sigma(\varepsilon_T)$ ,  $[\sigma(\varepsilon_L)]$  are the projection's errors.

Once a cut is made on the likelihood ratio, the  $J/\psi$ - $K$  invariant mass can be calculated for each candidate. In making the mass calculation the magnitude of the momenta of the muons are fitted by constraining the  $J/\psi$  mass to be the value given by the PDG [10]. The resulting  $B^+$  mass distribution can be seen in Fig. 1. The solid curve shows the results of an unbinned likelihood fit to signal  $J/\psi K^+$  and  $J/\psi\pi^+$ , plus  $J/\psi K^{*+}$  and combinatorial (an exponential function) backgrounds. The signal mass peaks contain  $23,287 \pm 344$  events.

For  $B^+$  meson candidates with mass in the range  $5.19 < M(B^+) < 5.36 \text{ GeV}/c^2$ , an additional track with charge opposite that of the  $B^+$  and  $p_T$  above  $0.75 \text{ GeV}/c$  is selected to be combined with the  $B$  in the search for excited  $B_j$  states  $B_1$  or  $B_2^*$ . Since  $B_j$  states decay via either strongly or electromagnetically their decay point is at the primary interaction vertex. Thus a significance  $S_\pi$  for the additional charged track to have come from the primary vertex is required. For these events the mass difference  $\Delta M = M(B^+\pi^-) - M(B^+)$  is computed with the result shown in Fig. 2. Since the photon in (1) and (2) is not reconstructed we expect to see three mass peaks from (1), (2) and (3)

with central positions:  $\Delta_1 = M(B_1) - M(B^*)$  for the decay of  $B_1 \rightarrow B^* \pi$ ,  $\Delta_2 = M(B_2^*) - M(B^*)$  for the decay  $B_2^* \rightarrow B^* \pi$  and  $\Delta_3 = M(B_2^*) - M(B)$  for the decay  $B_2^* \rightarrow B \pi$ .

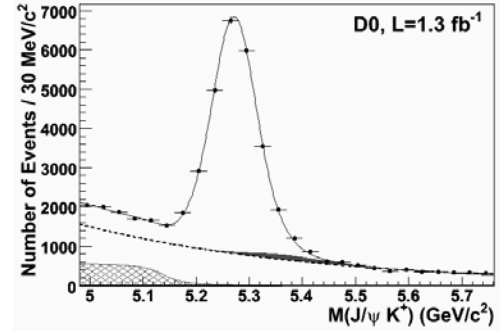


FIG. 1 Invariant mass for  $J/\psi K^+$  events. The solid line is the fit to signal plus background (see text). The separate contributions from  $J/\psi \pi^+$  (solid filled),  $J/\psi K^{*+}$  (cross-hatched) and combinatorial (dashed line) backgrounds are also shown.

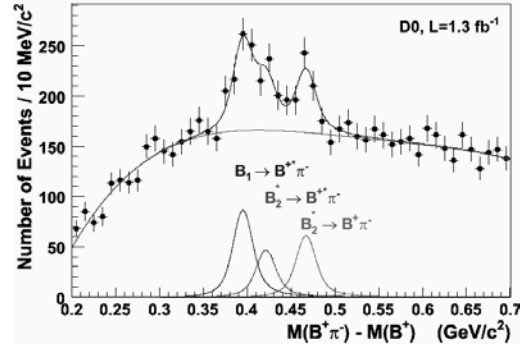


FIG. 2 Invariant mass difference  $\Delta M = M(B^+\pi^-) - M(B^+)$  for the  $B^+\pi^-$  candidates. The three peaks for the three decays given in equations (1), (2) and (3) are shown.

These peaks are seen in Fig. 2. Note that  $\Delta_2 = \Delta_3 - [M(B^*) - M(B)] = \Delta_3 - 45.78 \text{ MeV}/c^2$  [11]. The expected distribution in Fig. 2 is then fitted as follows:

$$(4) F(\Delta M) = F_{\text{sig}}(\Delta M) + F_{\text{bckg}}(\Delta M) \text{ where } F_{\text{sig}}(\Delta M)$$

contains the convolution of a relativistic Breit-Wigner with the experimental mass resolution and variable fractions that yield the proportionate amounts  $f_1$  and  $f_2$  for the fractions of  $B_1$  in the  $B_j$  signal and  $B_2^* \rightarrow B^* \pi$  in the  $B_2^*$  signal. The convolution of the Breit-Wigner and the Gaussian resolution in  $\Delta M$  take into account experimental resolu-

tion and the threshold effects [12] for  $L = 2$  decay. The background term  $F_{\text{bckg}}(\Delta M)$  is a 4<sup>th</sup> order polynomial. The natural widths,  $\Gamma_1$  and  $\Gamma_2$  of the two states are narrower than the experimental mass resolutions and are thus set to  $10 \text{ MeV}/c^2$  in the fit. The fit yields :

$$M(B_1) - M(B^+) = 441.5 \pm 2.4 \pm 1.3 \text{ MeV}/c^2, \text{ and}$$

$$M(B_2^*) - M(B_1) = 26.2 \pm 3.1 \pm 0.9 \text{ MeV}/c^2.$$

Here the first error is statistical and the second is systematic. Taking into account the correlation between these two measurements,  $-0.659$ , and using the mass of the  $B^+$  the absolute  $B_1$  and  $B_2^*$  masses are:

$$M(B_1) = 5720.6 \pm 2.4 \pm 1.4 \text{ MeV}/c^2, \text{ and}$$

$$M(B_2^*) = 5746.8 \pm 2.4 \pm 1.7 \text{ MeV}/c^2.$$

The number of  $B_J$  decays is found to be  $662 \pm 91$ .

Table 1 shows how the fit chi-squared varies with the number of peaks that are fitted.

Table 1. Mass Distribution Fitting Results		
Hypothesis	No. of Deg. Freedom	Chi-sq.
3 peaks	40	33
2 peaks; No $B_2^*$ to $B^* \pi$	41	41
1 pk, floating $\Gamma$	42	54
No B-W peaks	45	97

Inspection of Table 1 shows that although three peaks are preferred the statistical significance is marginal. Theory[13],[14] predicts that  $B_2^*$  should decay with nearly equal branching ratios into  $B\pi$  and  $B^* \pi$ , which the fitted three peak hypothesis prefers.

The number of  $B_J$  mesons and the fitted values of the fractions  $f_1$  and  $f_2$  can be used to determine the production and decay ratios of  $B_1$  and  $B_2^*$  if the efficiencies for selecting an additional pion are determined by simulation for the decays:

$$B_1 \rightarrow B^* \pi, B_2^* \rightarrow B^* \pi \text{ and } B_2^* \rightarrow B \pi.$$

The respective efficiencies:  $\varepsilon_1$ ,  $\varepsilon_2$  and  $\varepsilon_3$  are determined separately by simulation for each of the decay modes (1) – (3). The resultant production and decay ratios are:

$$R_1 = \frac{Br(B_1 \rightarrow B^{*+} \pi)}{Br(B_J \rightarrow B^{(*)} \pi)} = 0.477 \pm 0.069 \pm 0.062,$$

$$R_2 = \frac{Br(B_2^* \rightarrow B^* \pi)}{Br(B_2^* \rightarrow B^{(*)} \pi)} = 0.475 \pm 0.095 \pm 0.069,$$

$$R_J = \frac{Br(b \rightarrow B_J^0 \rightarrow B^{(*)} \pi)}{Br(b \rightarrow B^+)} = 0.139 \pm 0.019 \pm 0.032.$$

The overall efficiency for detecting an additional pion for any of the  $B_J \rightarrow B^{(*)} \pi^- = 0.342 \pm 0.008 \pm 0.028$ . The result for  $R_J$  takes into account the decay  $B_J \rightarrow B^0 \pi^0$  assuming isospin symmetry. The production and decay ratios for the three peak hypothesis agree well with predictions and give added confidence that the three peak interpretation is correct.

#### 4. The orbitally-excited neutral $B_{s2}^*$ meson

In addition to the  $\bar{b}d$  quark states discussed above we have searched for  $\bar{b}s$  type states. In the heavy quark effective theory nomenclature, the heavy quark decouples from the light quark and the orbitally excited  $L = 1$  light quark states have total angular momentum  $j_q = 1/2$  or  $3/2$ . When the heavy quark spin is combined with the  $j_q$  light quark angular momentum four states are formed from the two  $j_q$  doublets to give four hyperfine states with two  $j_q = 1/2$  states named  $B_{s0}^*$  and  $B_{s1}$  and two  $j_q = 3/2$  states:  $B_{s1}$  and  $B_{s2}^*$ .

If all four states are kinematically allowed they are expected to decay predominantly to  $B^*K$  or  $BK$ .

$$(5) B_{s1} \rightarrow B^{*+} K^-; \quad B^{*+} \rightarrow B^+ \gamma;$$

$$(6) B_{s2}^* \rightarrow B^{*+} K^-; \quad B^{*+} \rightarrow B^+ \gamma;$$

$$(7) B_{s2}^* \rightarrow B^+ K^-.$$

The analysis in this search parallels the search described in the previous section. The data set is essentially the same with same conditions for the selection of the  $J/\psi$ , that decays to  $\mu^+ \mu^-$  and the  $K^+$  that make the  $B^+$  meson. For each reconstructed  $B^+$  candidate with mass  $5.19 < M(B^+) < 5.36 \text{ GeV}/c^2$ , an additional track, assumed to be a  $K$  meson, with charge opposite that of the  $B^+$ , is selected if its transverse momentum is  $> 0.6 \text{ GeV}/c$ . This  $B^+$  selection results in  $20,915 \pm 293$  events. Since the

$B_{sJ}$  mesons decay at the primary vertex production point a significance  $S$ , on the normalized length projection of the charged  $K < \sqrt{6}$  is required.

In the  $B^{*+}$  decays the 45.8 MeV photon is not detected, which shifts the mass difference of the reconstructed  $B_s$ ,  $\Delta M = M(B^+ K^-) - M(B^+) - M(K^-)$ , down by  $E_\gamma = 45.78 \pm 0.35 \text{ MeV}/c^2$ . The  $\Delta M$  distribution is shown in Figure 3. The three possible decays (4) through (6) will not all occur if the mass of the decay products exceeds the resonance mass.

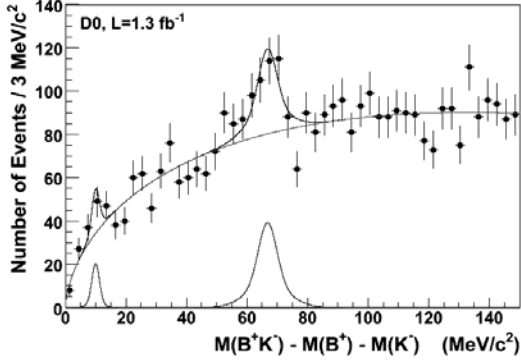


FIG. 3: Invariant mass difference  $\Delta M = M(B^+ K^-) - M(B^+) - M(K^-)$ . Curves represent fitted background and signal described in the text.

Fig. 3 shows a region around  $67 \text{ MeV}/c^2$  where there is an event excess above background. Neglecting the small possible peak at  $\sim 10 \text{ MeV}/c^2$ , the main peak and background are fitted with eq. (4) where

$$F_{sig}(\Delta M) = N \cdot Res(\sigma_1, \sigma_2, S, \Delta, \Delta M).$$

In this expression,  $\Delta$  is the mass of the resonance,  $M(B_{s2}^*) - M(B^+) - M(K^-)$  and  $N$  is the number of  $B_{s2}^* \rightarrow B^+ K^-$  decays. The background is fitted as a modified power-law function:

$$F_{bckg}(\Delta M) = c \cdot (\Delta M)^k + d \cdot \Delta M,$$

where  $c$ ,  $k$  and  $d$  are fitted parameters. The detector resolution,  $Res(\sigma_1, \sigma_2, S)$  is determined by Monte Carlo simulation that includes a relativistic Breit-Wigner function convolved with two Gaussians, with  $\sigma_1, \sigma_2$  equal to  $2.7$  and  $6.2 \text{ MeV}/c^2$ , respectively, that describe the mass measurement resolution and  $S$  is the relative normalization of the narrow to wide Gaussians; i.e., the height of the narrow Gaussian is  $S = 1.2$  times the height of the wide Gaussian. Studies of  $B^+ \rightarrow J/\psi K^+$  and  $D^{*+} \rightarrow D^{*0} \pi^+$  show the simulation underestimates the data mass resolution by  $\sim 10\%$ , so the widths of the Gaussians are increased by  $10\%$  with an error estimate of  $100\%$  applied to this correction.  $\Gamma$  in the Breit-Wigner fit

to the resonance is convolved with the detector resolution in the fitting of the signal and background. The following parameters result from the fit:

$$\Delta = 66.7 \pm 1.1 \text{ (stat.) MeV}/c^2, \text{ and}$$

$$N = 141 \pm 28 \text{ (stat.) events.}$$

The  $\chi^2/\text{d.o.f.}$  of the fit is  $50/45$ . Without the  $B_{s2}^*$  the  $\chi^2/\text{d.o.f.}$  increases to  $77/47$ , which implies the resonance is established with a statistical significance of greater than  $5\sigma$ .

Using the PDG values of the  $B^+$  ( $5279.1 \pm 0.5 \text{ MeV}/c^2$ ) and  $K^-$  ( $493.677 \text{ MeV}/c^2$ ) masses as input and also making a slight correction to the D0 momentum scale (from studies of large  $J/\psi \rightarrow \mu\mu$  samples) of  $+0.07 \text{ MeV}/c^2$  we find:

$$M(B_{s2}^*) = 5839.6 \pm 1.1 \text{ (stat.)} \pm 0.7 \text{ (sys.) MeV}/c^2.$$

This measurement agrees with CDF's published value of  $5839.7 \pm 0.7 \text{ MeV}/c^2$  [15]. The event yield of  $141 \pm 28$  candidates and the number of  $B^+ 20915 \pm 293$  are used to calculate the relative production rate in the formula:

$$R_J = \frac{Br(b \rightarrow B_{s2}^* \rightarrow B^+ K^-)}{Br(b \rightarrow B^+)} = \frac{N(B_{s2}^*)}{N(B^+) \cdot \epsilon} = (1.15 \pm 0.23 \pm 0.13) \%$$

Here  $\epsilon$  is the relative detection efficiency for  $B_{s2}^*$  events compared to  $B^+$  events; it is the efficiency to select an additional  $K$  meson and is determined by simulation to be  $= 0.518 \pm 0.011$ . The simulation emphasizes matching the transverse momentum distributions in the simulation with those in the data.

Theory predicts that the  $B_{s2}^*$  should decay equally to  $B_{s2}^+ K^-$  and  $B^+ K^-$ . Since the mass difference in the  $B_{s2}^+ K^-$  mode is small, its rate is expected to be suppressed by a factor  $(p^*/p)^5$ , where  $p^*$  ( $p$ ) is the center of mass momentum of the  $K$  meson in the decay  $B_{s2}^* \rightarrow B_{s2}^+ K^-$  ( $B^+ K^-$ ). With the  $B_{s2}^*$  mass reported here a suppression of  $0.074$  is calculated so no  $B_{s2}^* \rightarrow B_{s2}^+ K^-$  observation is expected in the  $\Delta M$  distribution for this decay mode.

Regarding a possible low-mass bump in Fig. 3 at  $\Delta M \sim 10 \text{ MeV}/c^2$ , CDF has reported the observation [16] of a state interpreted to be the  $B_{sJ}$  that de-

cays to  $B^{*+} K^-$  at  $10.73 \pm 0.21(\text{stat.}) \pm 0.14 \text{ MeV}/c^2$ . To test for the presence of this in our data, a two peak hypothesis is postulated in our  $\Delta M$  fit, with both narrow and wide double Gaussians for both peaks, following the discussion in the previous section for a single resonance fit. The resulting fit is shown in Fig. 3 with the following parameters:

$$\begin{aligned} \Delta_1 &= M(B_{s1}) - M(B^{*+}) - M(K^-) \\ &= 11.2 \pm 1.6 (\text{stat.}) \text{ MeV}/c^2, \text{ and} \\ N &= 22 \pm 15 (\text{stat.}) \text{ events.} \end{aligned}$$

The  $\chi^2 / \text{d.o.f.}$  is 46/43 and without the  $B_{s1}$  it increases to 50/45 which implies a statistical significance of less than  $2\sigma$  for the presence of the  $B_{s1}$  in our data. Thus, the data presented here can neither confirm nor deny the existence of the  $B_{s1}$ . More details[17] on this result can be found in the cited reference.

## 5. The Cascade-b Baryon: $\Xi_b$

Because the Tevatron provides hadrons of sufficient energy, hitherto undiscovered high-mass b-quark states are the subject of particle searches. The ability to produce many different b-states in abundance brings with it the choice of triggers that can be used to facilitate success in new searches. We learned in the case of the  $\Lambda_b$  that the decay mode:  $J/\psi + \Lambda$  with the  $J/\psi \rightarrow \mu^+ \mu^-$  and  $\Lambda \rightarrow p \pi^-$  provided a good sample of data using a di-muon trigger. This same scheme was applied in the case of the cascade-b since it decays to a  $J/\psi + \Xi^-$  that then decay to  $\mu^+ \mu^-$  and  $\Lambda \pi^-$ , respectively.

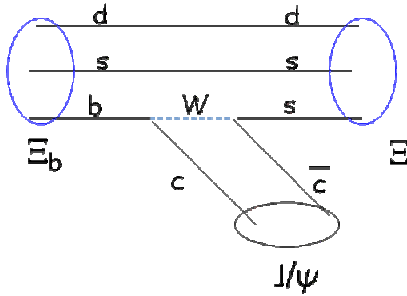


FIG. 4. Feynman diagram that represents the basis for establishing the event sample used in the cascade-b analysis.

Because the  $\Xi^-$  and  $\Lambda$  are both rather long-lived weak decays it was necessary to extend the track search fiducial volume for efficiently finding their decay products to establish the  $\Xi_b$  candidate event sample. To establish efficient criteria PYTHIA Monte Carlo  $\Xi_b$  samples were generated and their decays were simulated with EVTGEN. The  $\Xi_b$  mass and lifetime chosen for the simulation were  $5.840 \text{ GeV}/c^2$  and  $1.33 \text{ ps}$ , respectively, as being representative of theoretical expectations. The MC events were passed through the D0 analysis suite of programs that use the GEANT package to simulate the D0 detector. To obtain the relevant  $p_t$  distributions for comparison of MC with data the MC events were reweighted by matching the  $p_t$  spectra of the distributions of the  $J/\psi$ , proton and pion as determined in an independent study of a  $\Lambda_b$  event sample.

$J/\psi \rightarrow \mu^+ \mu^-$  decays were reconstructed using the standard D0 packages from tracks in the muon system and calorimeters, with the required matching in central tracking and muon detectors. The two opposite signed muons were required to have  $p_t > 1.5 \text{ GeV}/c$  and at least one muon was required to be reconstructed in three muon drift tube layers. The di-muon invariant mass was required to be in the mass range 2.5 to  $3.6 \text{ GeV}/c^2$ . Events with  $J/\psi$  candidates were reprocessed using track reconstruction code with high efficiency for low  $p_t$  or a large impact parameter with respect to the primary vertex of the event. The efficiencies for reconstruction of the  $(\Lambda, \pi^-)$  combinations in the  $\Xi^-$  candidate sample, shown in Fig. 5, increased more than 5-fold with reprocessing.

The  $\Lambda \rightarrow p \pi^-$  (charge conjugate states are implied with anti-particles as expected) was formed from opposite charged track candidates with a common vertex. The highest  $p_t$  track, of the pair, was taken to be the (anti-)proton as preferred by MC. The assembled  $\Lambda$  mass was required to be in the range  $1.105$  to  $1.125 \text{ GeV}/c^2$ . Both tracks had to have two or fewer hits in tracking detectors upstream of the  $\Lambda$  vertex and the impact parameter significance (impact parameter divided by its error) had to exceed three for one of the tracks and four for the other track.

The  $\Lambda$  was combined with the negatively charged pion from the  $\Xi^-$ ,  $\Lambda, \pi^-$  vertex to make the  $\Xi^-$ . The two pions, one from the  $\Lambda$  decay and the other from the  $\Xi^-$  decay were required to have the same charge

(right-sign). Opposite charge combinations, such as  $\Lambda\pi^+$  formed a wrong-sign background sample. The invariant mass for both the wrong and right-sign  $\Lambda\pi$  combinations are shown in Fig. 5. The  $\Xi^-$  mass peak (right-sign) is shown along with the wrong-sign background which matches almost perfectly with no further normalization. A  $(\Lambda\pi^-)$  combination is considered to be a  $\Xi^-$  candidate if its mass is in the range  $1.305 < M(\Lambda\pi^-) < 1.340 \text{ GeV}/c^2$ .

The  $\Xi_b$  candidate masses were then calculated assuming they came from the  $(\Xi^-, J/\psi)$  combinations that originate from a common vertex and have an opening angle in the transverse plane of less than  $90^\circ$ . After imposing a proper decay length uncertainty cut of the  $J/\psi \Xi$  transverse vertex of  $< 0.5\text{mm}$ , a total of 2308 events remain. Wrong-sign events selected with the same criteria result in 1124 events in the control sample.

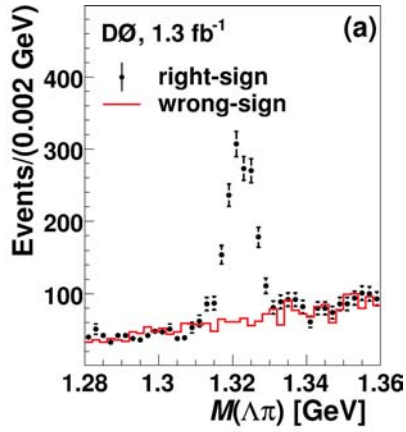


FIG. 5. Invariant mass of the right-sign  $\Lambda\pi^-$  and wrong-sign  $\Lambda\pi^+$  combinations after reprocessing. A fit that includes a Gaussian for the  $\Xi^-$ 's and a first order polynomial for the background yields  $603 \pm 34 \Xi^-$ 's and  $548 \pm 31 \Xi^+$ 's.

It is still necessary to suppress background using the distinguishing features of the  $\Xi_b$  MC events and the wrong-sign background. Protons and pions from the  $\Xi_b$  decay chain have higher momenta than those from the backgrounds. Studies show that requiring protons to have  $p_t > 0.7 \text{ GeV}/c$  and pions from the  $\Lambda$  and  $\Xi$  to have  $p_t > 0.3$  and  $0.2 \text{ GeV}/c$ , respectively, reduce the wrong-sign background by 91.6% while keeping 68.7% of the MC  $\Xi_b$  signal events. Back-

grounds such as charged and neutral B decays to  $J/\psi K^*$  and to  $J/\psi K^*\pi$  are suppressed by requiring the  $\Xi^-$  candidate decay lengths to be greater than  $0.5 \text{ cm}$  and the cosine of the colinearity angle between the  $\Xi^-$  direction and the direction from the  $\Xi^-$  production vertex to its vertex in the transverse plane, to be  $> 0.99$ . These two requirements reduce the background by 56.4% and remove only 1.7% of the MC signal. Since the  $\Xi_b$  is expected to have a lifetime that is larger than the sideband events (B decays), the transverse proper decay length significance is required to be greater than two. This final requirement keeps 83% of the MC signal while keeping only 44% of the background events.

After applying all of these cuts 51 events survive with  $\Xi_b$  masses between  $5.2$  and  $7.0 \text{ GeV}/c^2$ . This mass range was chosen to encompass all known b hadrons and the predicted  $\Xi_b$  masses. The mass for each event was calculated using:

$$(8) \quad M(\Xi_b) = M(\Xi^-, J/\psi) - M(\mu^+\mu^-) - M(\Lambda\pi^-) + M_{\text{PDG}}(J/\psi) + M_{\text{PDG}}(\Xi^-).$$

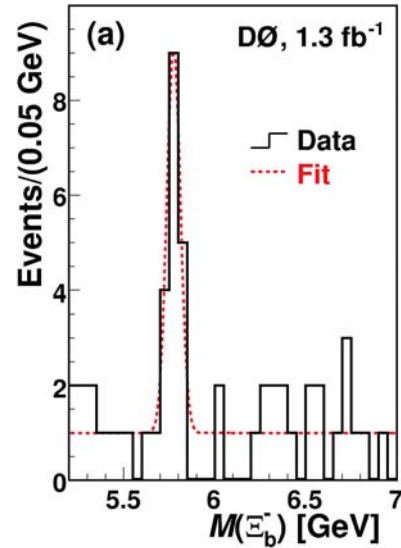


FIG. 6. The  $\Xi_b$  mass distribution is plotted after all selection criteria are applied. The dotted curve is an unbinned likelihood fit to a constant background plus a Gaussian signal in mass.

This method improves the measured  $\Xi_b$  mass resolution. The masses labeled PDG were taken from the Particle Data Group[10] listings. The mass distribu-

tion is shown in Fig. 6. A peak at  $\sim 5.8 \text{ GeV}/c^2$  is obvious.

Cross checks were performed to investigate the possibility that the observed peak is due to analysis techniques. In all, six checks were performed: (1) The  $J/\psi \Lambda \pi^+$  mass distribution of the wrong-sign events shows no more than two events in any mass bin where the bin size is the same as Fig.6. (2) The event selection is applied to the sidebands of the  $\Xi^-$  peak, while requiring  $1.28 < M(\Lambda \pi^-) < 1.36 \text{ GeV}/c^2$ , but excluding the  $\Xi^-$  mass window. No peaks appeared. Similarly the selection was applied to the sidebands of the  $J/\psi$  over the interval 2.5 to 2.7  $\text{GeV}/c^2$ . Such a test was not performed in the mass region above the  $J/\psi$  mass to avoid contamination from  $\psi'$  events. (4) The possibility that a fake signal was caused by residual b-hadron background was investigated by applying the final  $\Xi_b$  selection to high statistics MC samples of  $B^- \rightarrow J/\psi K^* \rightarrow J/\psi K_s \pi^-$ ,  $B^0 \rightarrow J/\psi K_s$  and  $\Lambda_b \rightarrow J/\psi \Lambda$ . None of these samples indicated any  $J/\psi \Xi^-$  mass peaks. (5) The mass distributions of the  $J/\psi$ ,  $\Xi^-$  and  $\Lambda$  were investigated by relaxing the mass requirements on these particles one at a time in the  $\Xi_b$  mass region and its sidebands. The numbers of these particles migrating in and out of the sidebands and signal regions is entirely consistent with expectations. (6) The robustness of the peak was tested by varying the selection criteria within reasonable ranges. All of these studies confirmed the peak at the same mass.

The  $\Xi_b$  candidate mass distribution is fitted to a resonance signal plus background using an unbinned likelihood method. The signal is assumed to be Gaussian and the background is taken as flat. The fitting results give a  $\Xi_b$  mass of  $5.774 \pm 0.011 \pm 0.015 \text{ GeV}/c^2$  with an rms width of  $0.037 \pm 0.008 \text{ GeV}/c^2$  and a yield of  $15.2 \pm 4.4$  events [18]. This result agrees with the CDF measurement of  $5.7929 \pm 0.0025 \pm 0.0017 \text{ GeV}/c^2$  [19]. The fitted mass of the MC generated  $\Xi_b$  events, using the same assumptions, is  $5.839 \pm 0.003 \text{ GeV}/c^2$ , which is in good agreement with the input value of  $5.840 \text{ GeV}/c^2$ . The fitted rms width is  $0.035 \pm 0.002 \text{ GeV}/c^2$ , which compares well with the data result.

The significance of the distribution is determined by calculating the likelihood for the signal plus background:  $\mathcal{L}_{s+b}$ . Then one calculates the likelihood  $\mathcal{L}_b$  for the background alone, and forms the logarithmic

likelihood ratio  $R = \sqrt{2 \ln (\mathcal{L}_{s+b} / \mathcal{L}_b)}$  which gives a statistical significance of  $5.5 \sigma$ . This corresponds to a probability of random occurrence from a background fluctuation of  $3.3 \times 10^{-8}$ . One can also calculate significance from the signal and background yields in the fitting process after invoking the systematic error of  $+1.9/-0.4$  events. This gives a minimum significance of  $5.3 \sigma$ .

The results presented here are the efforts of many colleagues whom we wish to acknowledge. These results are also in good agreement with other experiments and especially the CDF experiment at Fermilab. We would like to thank the organizers of the BEACH Conference whose efforts made our attendance at the meeting both worthwhile and pleasant.

## References

- 
- [1] T. Matsuki and T. Morii, Phys. Rev D **56**, 5646 (1997). T. Matsuki, T. Morii and K. Sudoh, Prog. Theor. Phys. **117**, 1077 (2007).
  - [2] M. Di Piero and E. Eichten, Phys. Rev. D **64** 114004 (2001).  
E. J. Eichten, C. T. Hill and C. Quigg, Phys. Rev. Lett. **71**, 4116 (1993).
  - [3] N. Isgur, Phys. Rev. D **57**, 4041 (1998).
  - [4] D. Ebert, V. O. Galkin, and R. N. Faustov, Phys. Rev. D **57**, 5663 (1998); **59**, 019902 (1998).
  - [5] A. H. Orsland and H. Hogaasen, Eur. Phys. J. C **9**, 503 (1999).
  - [6] A. Falk and T. Mehen, Phys. Rev. D **53**, 231 (1996).
  - [7] V. M. Abazov *et al.* (D0 Collaboration), Phys. Rev. Lett. **99**, 172001 (2007).
  - [8] J. Abdallah *et al.* (DELPHI Collaboration), Eur. Phys. J. C **32**, 185 (2004).
  - [9] G. Borisov, Nucl. Instrum. Methods Phys. Res., Sect. A **417**, 384 (1998).
  - [10] W.-M. Yao *et al.* (Particle Data Group), J. Phys. G **33**, 1 (2006).
  - [11] Ibid. Ref. 10, p. 803 (2006).
  - [12] J. Blatt and V. Weisskopf, *Theoretical Nuclear Physics* (John Wiley & Sons, New York, 1952, p. 361).
  - [13] M. Di Piero and E. Eichten, op cit. p. 114004 (2001) and E. J. Eichten, C. T. Hill and C. Quigg,, op cit. p. 4116 (1993).
  - [14] A. Falk and T. Mehen, op cit., p231(1996).
  - [15] T. Aaltonen *et al.* (CDF Collaboration) Phys. Rev. Lett. **100**, 082001(2008).

- 
- [16] I. V. Gorelov *et al*, arXiv:hep-ex/0610080v1  
27Oct2006.
- [17] V.M. Abazov *et al*. (D0 Collaboration), Phys.  
Rev. Lett. **100**, 082002 (2008).
- [18] V.M. Abazov *et al* (D0 Collaboration). Phys.  
Rev. Lett. **99**, 052001(2007).
- [19] T. Aaltonen *et al* (CDF Collaboration) Phys.  
Rev. Lett. **99** 052002(2007).